Metal-Ligand Interplay in Strongly Correlated Oxides: A Parametrized Phase Diagram for Pressure-Induced Spin Transitions

Aleksi Mattila,[1] Jean-Pascal Rueff,[2,3] James Badro,[4,5] György Vankó,[6,7] and Abhay Shukla[8]

[1]*Division of X-Ray Physics, Department of Physical Sciences, POB 64, 00014 University of Helsinki, Finland*
[2]*Laboratoire de Chimie Physique-Matière et Rayonnement, Université Pierre et Marie Curie, CNRS, 11 rue Pierre et Marie Curie, 75005 Paris, France*
[3]*Synchrotron SOLEIL, L'Orme des Merisiers, BP-48 Saint-Aubin, F-91192 Gif-sur-Yvette, France*
[4]*IMPMC, Université Pierre et Marie Curie, CNRS, F-75015 Paris, France*
[5]*Minéralogie, Institut de Physique du Globe de Paris, CNRS, F-75015 Paris, France*
[6]*European Synchrotron Radiation Facility, BP 220, F-38043 Grenoble, France*
[7]*KFKI Research Institute for Particle and Nuclear Physics, P.O. Box 49, H-1525 Budapest, Hungary*
[8]*Université Pierre et Marie Curie-Paris 6, UMR7590, IMPMC, 140 Rue de Lourmel, Paris, F-75015 France*

(Received 5 December 2006; published 9 May 2007)

We investigate the magnetic properties of archetypal transition-metal oxides MnO, FeO, CoO, and NiO under very high pressure by x-ray emission spectroscopy at the $K\beta$ line. We observe a strong modification of the magnetism in the megabar range in all the samples except NiO. The results are analyzed within a multiplet approach including charge-transfer effects. The spectral changes are well accounted for by changes of the ligand field acting on the d electrons and allows us to extract the d-hybridization strength, O-2p bandwidth and ionic crystal field across the magnetic transition. This approach allows first-hand insight into the mechanism of the pressure-induced spin transition.

DOI: 10.1103/PhysRevLett.98.196404 PACS numbers: 62.50.+p, 71.27.+a, 71.70.Ch, 78.70.En

Pressure is an effective means to drive the electronic density of a system, and thereby the electron interaction and delocalization. In correlated materials such as transition-metal oxides (henceforth MO), lattice compression strongly affects transport, structural, and magnetic properties, often leading to a magnetic collapse [1]. The latter is usually explained as a high-spin (HS) to low-spin (LS) transition on the metal ion site due to the competition between crystal-field and Hund coupling energies. Alternatively, the disappearance of the magnetic moment can be seen to result from the breakdown of the Stoner criterion. The vanishing magnetism then concurs with an insulator-metal transition, i.e., a closure of the correlation or charge-transfer gap in MO. A satisfactory description of the d electrons in MO constitutes, in fact, an ongoing challenge for the theory. This is all the more relevant for pressure-induced phenomena like magnetic collapse which need a proper treatment of d hybridization. Crystal-field theory was applied quite early to predict the magnetic transition pressures [2]. First-principle calculations can be also cited in this context: high-pressure magnetism of MO has been treated in a pure band approach [3] while effects of correlations were more recently included, mostly in iron compounds [4–8].

Recent advances in high-pressure spectroscopy and improvements in theoretical modeling of strongly correlated systems are now in a position to further current understanding. In this Letter we report the results of x-ray emission spectroscopy (XES) at the $K\beta$ line in a series of prototypical MO, MnO, FeO, CoO, and NiO under very high-pressure conditions. XES is now well established as a local probe of the transition-metal magnetism. It is an all-photon technique fully relevant to transition metals at high pressure, even though the use diamond anvil cells place limitations for the lowest emission energies. The data are analyzed in the light of multiplet calculations within the Anderson impurity model [9–11]. Here, in contrast to bandlike treatments of d electrons, crystal-field, ligand bandwidth, and charge transfer are explicit parameters providing a physically intuitive insight. The model, derived from the configuration interaction approach, was first introduced to explain the core-photoemission spectra of transition metals [12,13], and later extended to the $K\beta$ emission line in Ni-compounds [14] and MO [15–17]. The multiplet calculation scheme yields an accurate model of the emission line shape allowing a direct estimate of the fundamental parameters. In this Letter the method is applied to pressure-induced magnetic collapse, giving the opportunity to study the systems in two contrasting states from the electronic, magnetic, and even structural point of view. This allows us to establish the frontiers of a phase diagram characterizing this transition and shed new light on the intermediate pressure regime.

We have measured XES at the $K\beta$ line in MnO, FeO, CoO, and NiO at the European Synchrotron Radiation Facility using diamond anvil cells and a Be gasket [18,19]. The high-pressure FeO spectrum has been measured at the Advanced Photon Source using the setup described in Ref. [19]. The high-pressure spectra of FeO and CoO have been obtained after laser heating at high pressure. Figures 1(a)–1(d) summarizes the $K\beta$ emission spectra measured in the MO series at low and high pressures. The spectra are aligned to the main-peak energy and normalized to unity. They all present a satellite structure

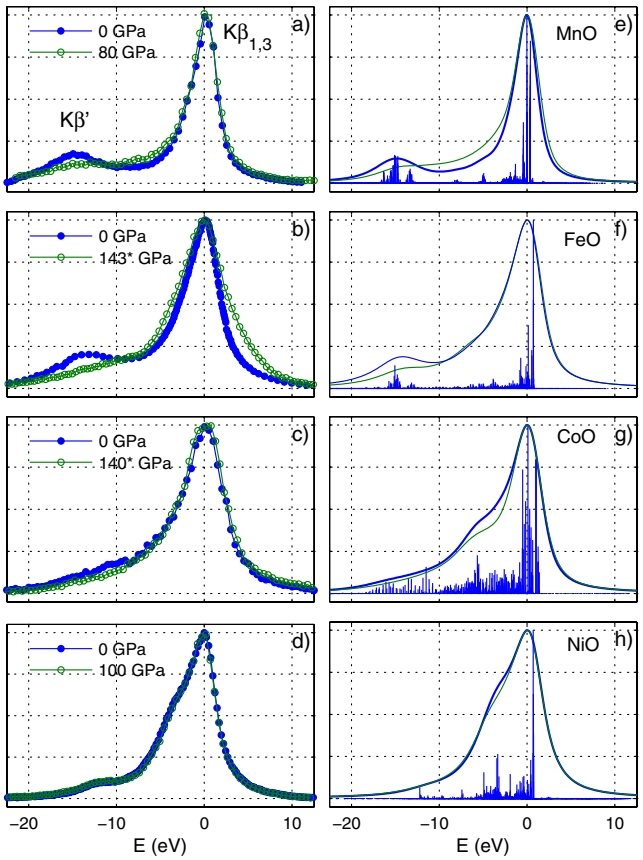

FIG. 1 (color online). (a)–(d) $K\beta$-XES spectra measured in MnO, FeO, CoO, and NiO in both ambient (blue closed circles) and high-pressure (green open circles) phases. (*) indicates spectra obtained after laser-heating. (e)–(h) Calculated spectra at ambient (blue lines) and high pressures (green thin lines). Ticks are raw ambient-pressure data before broadening. The spectra are normalized to the $K\beta_{1,3}$ peak height.

(known as $K\beta'$) peaking on the low energy side of the main emission line ($K\beta_{1,3}$). At high pressure, all the spectra but NiO show significant modifications in the line shape, essentially observed in the satellite region. The collapse of the satellite in MnO starts around 60 GPa and in CoO and FeO at about 140 GPa following a laser heating [18,20]. The asymmetric broadening of the main line in FeO at 140 GPa is an artifact due to different experimental setups.

Following the the treatment of Peng *et al.* [21] within the atomic multiplet formalism, the main line and satellite result from the exchange interaction between the $3p$ core hole and the $3d$ orbital in the final state, which splits the final state manifold. As a rule of thumb, the satellite is therefore expected to shrink with decreasing $3d$ magnetic moment and to move closer to the main peak. This agrees well with the observed spectral changes when going from MnO ($3d^5$, $S = 5/2$) to NiO ($3d^8$, $S = 1$). It also qualitatively accounts for the collapse of the satellite at high-pressure observed in MnO, FeO and CoO, viewed as the signature of the HS to LS transition on the given metal ion. The nearly identical spectra in NiO, where no such transition is expected, confirms the rule.

The modification of the electronic properties at high pressure accompanying the magnetic collapse is usually escorted by a structural transition. Which of the structural or magnetic transition initiates the other is beyond discussion here, without structural refinement under pressure. But the tight correlation between the phenomena remains and can serve to fingerprint the phase transition (cf. Ref. [3]). As a matter of fact, our results consistently confirm the known structural pressure transitions in MnO (80–90 GPa) [22], FeO (90–100(140) GPa) [22,23], and CoO (90–100 GPa) [24], whereas none is observed in NiO up to 140 GPa [25].

The atomic description of XES, however, omits the crucial role played by the O($2p$)-M($3d$) charge-transfer effects and finite O-$2p$ bandwidth. Inclusion of the charge-transfer in the multiplet calculations also substantially improves the simulated main-peak to satellite intensity ratio, via a transfer of spectral weight to the main peak [14]. In the cluster model charge transfer enters the calculations through a configuration interaction scheme within the single impurity Anderson model [26]. We considered a linear combination of $3d^n$, $3d^{n+1}\underline{L}$, and $3d^{n+2}\underline{L}^2$ configurations, where $\underline{L}$ denotes a hole in the O-$2p$ state, for CoO ($n = 7$) and NiO ($n = 8$) ground states. Two configurations $3d^n$ and $3d^{n+1}\underline{L}$ were used for MnO ($n = 5$) and FeO ($n = 6$). The calculations were made in the O_h basis set at 300 K. The Slater integrals and spin-orbit parameters were calculated using the Hartree-Fock method [27], and the Slater integrals were further scaled down to 80% to account for the intra-atomic configuration interaction effects. Crystal-field effects were considered using the approach developed by Butler [28] and charge-transfer effects using the code by Thole and Ogasawara [10].

The model parameters were first chosen to reproduce the emission spectra at ambient pressure. The parameters, charge-transfer energy Δ (defined as the energy difference between the centers of gravities of $3d^n$ and $3d^{n+1}\underline{L}$ configurations), hybridization strength in the ground state V_{e_g}, the O-$2p$ bandwidth W, and the crystal-field splitting 10Dq are summarized in Table I. In addition, the on-site Coulomb interaction U in CoO and NiO was set to 6.0 and 8.2 eV, respectively. We used the same core hole Coulomb interaction U_{dc} for both $1\underline{s}$ and $3\underline{p}$ core hole states. The hybridization strength for t_{2g} symmetry states $V_{t_{2g}}$ was set to half of the value for e_g states V_{e_g} and for core hole states V_{e_g} was reduced by 0.4 eV from the ground state value. The term dependence of the final state lifetime broadening was approximated using the same linear dependence [$-0.2 \times \omega$ full width at half maximum (FWHM)] of the broadening on the fluorescence emission energy ω for all the MO emission spectra [29]. The spectra were finally convoluted with a 1.5 eV FWHM Gaussian to account for the instrumental broadening. For the high-pressure emission spectra Δ, V_{e_g}, 10Dq, and W were adjusted to fit the calculated spectra to the experiment, while keeping the core hole

TABLE I. Parameters used in the calculations (in eV). The ground state configuration (HS/LS) is given in parentheses after the pressure value. For NiO with $3d^8$ configuration, no spin transition will occur in O_h local symmetry. Charge-transfer energy is given by Δ, V_{e_g} is the hybridization strength, 10Dq the crystal-field splitting, U_{dc} the core hole Coulomb interaction, and W denotes the oxygen $2p$ bandwidth.

	P (GPa)	Δ	V_{e_g}	10Dq	U_{dc}	W (O-$2p$)
MnO	0 (HS)	5.0	2.2	1	10.0	3.0
	80 (LS)	6.0	3.06	1.6	10.0	4.0
	100 (LS)	6.0	3.7	2.3	10.0	6.0
FeO	0 (HS)	5.0	2.4	0.5	7.0	5.0
	140 (LS)	5.0	3.2	0.8	7.0	9.0
CoO	0 (HS)	6.5	2.5	0.7	7.0	4.0
	140 (LS)	6.5	4.2	1.2	7.0	8.0
NiO	0	3.5	2.4	0.3	9.0	5.0
	100	4.5	3	0.65	9.0	7.5

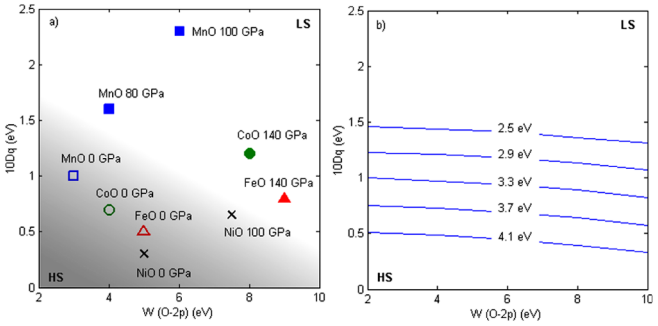

FIG. 2 (color online). Phase diagram of the magnetic collapse in the transition-metal oxides. (a) The symbol coordinates refer to calculated values of 10Dq and W (O-$2p$), for the HS (open symbols) and LS (closed symbols) states. Crosses indicate the absence of spin transition. The shaded area is a guide to the eyes separating the two regions. (b) The lines mark the calculated HS-LS transition boundary for d^7 configuration for different values of V_{e_g} shown in the figure. Charge-transfer energy Δ was set to 6.5 eV.

potentials and Slater integrals at ambient-pressure values [30]. The results are given in Table I. In CoO and NiO also the on-site Coulomb interaction U could be extracted as a parameter from the fit, yielding values of 6.0 and 9.2 eV, respectively. As the emission line shape is not very sensitive to small changes in the local symmetry, we used the O_h basis set at all pressures to reduce the number of model parameters, although some deviations from the octahedral symmetry occur in the high-pressure crystal phases. Figures 1(e)–1(h) show the calculated spectra for both the ambient and high-pressure phases. The result for the 100 GPa phase in MnO, calculated using the exprimental spectra from [31] as a reference, is shown in Fig. 3. The degree to which the experimental data can be reproduced is very good considering the simplicity of the model used, with the biggest difference being the overestimated shoulder intensity about 5 eV below the main line in CoO. This assures us that the parameters singled out by our approach are the relevant ones for the description of the magnetic collapse. For MnO, CoO, and FeO the calculations for the high-pressure phases yield a LS ground state and for ambient pressures a HS ground state. For NiO with $3d^8$ configuration, no spin transition occurs in O_h local symmetry.

Our findings, relating parameter values to the spin state of the system are summarized in Fig. 2. The role of these parameters taken separately has been emphasized in earlier approaches; that of the crystal-field splitting 10Dq being paramount in the atomic description of XES and relevant for dilute systems while bandlike calculations obviously take into account the O-$2p$ bandwidth W. Here we explicitly show the HS-LS transition as resulting from the conjugated effects of increase of the crystal-field splitting 10Dq *and* a broadening of the O-$2p$ bandwidth W together with the covalent contribution from the hybridization to the ligand field [11] at high pressures. While the increase of 10Dq clearly drives the system towards a LS state our analysis nicely highlights the interplay of the ligand bandwidth together with the hybridization. Figure 2(a) shows the calculated values of 10Dq and W for the four oxides across the magnetic transition. Both quantities increase to produce magnetic collapse though in varying proportions according to the system in question. This variation allows us to establish a rough frontier between the HS and LS states as shown by the difference in shading in the figure. The sizeable increase of 10Dq in MnO with pressure contrasts with the other oxides where it is smaller, the essential increase being in the oxygen bandwidth W [cf. Fig. 2(a)], which would tend to drive the oxides towards a metallic ground state [32]. This possibly explains the larger volume compressibility of MnO compared to FeO, CoO, and NiO [22,24,25,33], and the high-pressure transition towards the $B8$ compact structure. The effect of simultaneous evolution of these parameters together with hybridization across the magnetic collapse transition is represented in Fig. 2(b). The lines mark the calculated HS-LS transition boundary for the different values of V_{e_g} for a d^7 configuration. The increase of bandwidth W contributes to the stabilization of the LS ground state in addition to the effect of hybridization.

We can ask ourselves if this HS/LS transition is abrupt and to what degree the frontier between the two regions is well marked. As an example we show in Fig. 3 the emission line in MnO at four pressure points across the magnetic transition (circles). In addition to our data set (0, 11, 60, and 80 GPa), spectra from Ref. [31] measured at 80 GPa (to verify consistency) and 100 GPa (dashed line) were used. The calculated spectra (red solid line) at intermediate pressures were obtained by fitting a linear combination of the theoretical HS (0 GPa) and LS (100 GPa) spectra to the experiment. The weight of the HS state derived from the fit is indicated in the inset. The Mn spin state gradually decreases from ambient to the high pres-

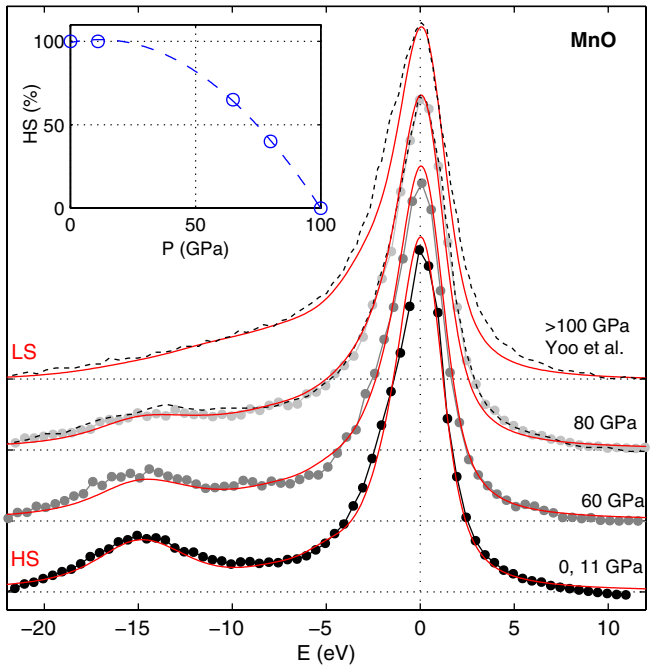

FIG. 3 (color online). XES spectra in MnO (circles) as a function of pressure. Data from Ref. [31] are shown with dashed lines at 80 and 100 GPa. Solid red lines are the calculated spectra. The intermediate pressure points have obtained from a linear combination of the HS and LS (100 GPa) spectra. The amount of spin state is indicated in the inset; the dashed line is a guide to the eyes.

sure, supposedly reaching a full LS state around 100 GPa which coincides with the reported Mott pressure transition [34]. The predicted moment in the metallic phase is $\sim 1\mu_B$ [3] in good accordance with a pure LS configuration. Thus the transition is characterized by an intermediate regime with both HS and LS states coexisting on the same site. Indeed, the computed energy separation between the HS and LS multiplets in MnO at 80 GPa is 12 meV, indicating that the HS state can be thermally populated although it does not constitute the true ground state. As pressure is increased, the population of the two states is progressively reversed, leading to full LS conversion eventually. An increase in temperature would further broaden the pressure range of this intermediate regime [8,35]. In other words, the sluggishness of the magnetic transition potentially results from a superposition of HS and LS states. The sluggish transition is a widely observed feature in transition-metal compounds, both in the magnetic (e.g., see [23,36]) or structural data. Possibly the sluggishness of the electronic transition is further enhanced through the interplay with the ligand as seen in Fig. 2(b), where large changes in W are needed to bring about changes in the magnetic state. In pure Fe, on the contrary, a sharp transition is observed [37].

A. M. has been supported by the Academy of Finland (Contract No. 201291/205967/110571). We thank the GSECARS beam line staff at APS for help during the FeO experiment and A. Kotani for discussions.

[1] H. G. Drickamer, C. W. Frank, and C. P. Slichter, Proc. Natl. Acad. Sci. U.S.A. **69**, 933 (1972).
[2] S. Ohnishi, Phys. Earth Planet. Inter. **17**, 130 (1978).
[3] R. E. Cohen, I. I. Mazin, and D. G. Isaak, Science **275**, 654 (1997).
[4] S. A. Gramsch, R. E. Cohen, and S. Y. Savrasov, Am. Mineral. **88**, 257 (2003).
[5] M. Cococcioni, A. D. Corso, and S. de Gironcoli, Phys. Rev. B **67**, 094106 (2003).
[6] X. Jiang and G. Y. Guo, Phys. Rev. B **69**, 155108 (2004).
[7] G. Rollmann, A. Rohrbach, P. Entel, and J. Hafner, Phys. Rev. B **69**, 165107 (2004).
[8] T. Tsuchiya, R. M. Wentzcovitch, C. R. S. da Silva, and S. de Gironcoli, Phys. Rev. Lett. **96**, 198501 (2006).
[9] A. Kotani and S. Shin, Rev. Mod. Phys. **73**, 203 (2001).
[10] F. M. F. de Groot, Chem. Rev. **101**, 1779 (2001).
[11] F. M. F. de Groot, J. Electron Spectrosc. Relat. Phenom. **67**, 529 (1994).
[12] J. Zaanen, C. Westra, and G. A. Sawatzky, Phys. Rev. B **33**, 8060 (1986).
[13] T. Mizokawa *et al.*, Phys. Rev. B **49**, 7193 (1994).
[14] F. M. F. de Groot, A. Fontaine, C. C. Kao, and M. Krisch, J. Phys. Condens. Matter **6**, 6875 (1994).
[15] T. A. Tyson *et al.*, Phys. Rev. B **60**, 4665 (1999).
[16] P. Glatzel, U. Bergmann, F. de Groot, and S. Cramer, Phys. Rev. B **64**, 045109 (2001).
[17] P. Glatzel *et al.*, J. Am. Chem. Soc. **126**, 9946 (2004).
[18] J.-P. Rueff *et al.*, J. Phys. Condens. Matter **17**, S717 (2005).
[19] J. Badro *et al.*, Phys. Rev. Lett. **89**, 205504 (2002).
[20] J. Badro *et al.*, Phys. Rev. Lett. **83**, 4101 (1999).
[21] G. Peng *et al.*, Appl. Phys. Lett. **65**, 2527 (1994).
[22] Z. Fang, I. Solovyev, H. Sawada, and K. Terakura, Phys. Rev. B **59**, 762 (1999).
[23] M. P. Pasternak *et al.*, Phys. Rev. Lett. **82**, 4663 (1999).
[24] Q. Guo *et al.*, J. Phys. Condens. Matter **14**, 11 369 (2002).
[25] T. Eto *et al.*, Phys. Rev. B **61**, 14 984 (2000).
[26] P. W. Anderson, Phys. Rev. **115**, 2 (1959).
[27] R. D. Cowan, *The Theory of Atomic Structure and Spectra* (University of California, Berkeley, 1981).
[28] P. Butler, *Point Group Symmetry Applications: Methods and Tables* (Plenum, New York, 1981).
[29] M. Taguchi, T. Uozumi, and A. Kotani, J. Phys. Soc. Jpn. **66**, 247 (1997).
[30] For NiO we first estimated 10Dq using a bond length dependence 10 Dq $\propto r^{-5}$ and after that we adjusted Δ, V_{e_g}, W, and U.
[31] C. S. Yoo *et al.*, Phys. Rev. Lett. **94**, 115502 (2005).
[32] A. Shukla *et al.*, Phys. Rev. B **67**, 081101 (2003).
[33] T. Kondo *et al.*, J. Appl. Phys. **87**, 4153 (2000).
[34] J. R. Patterson *et al.*, Phys. Rev. B **69**, 220101 (2004).
[35] W. Sturhahn, J. M. Jackson, and J.-F. Lin, Geophys. Res. Lett. **32**, L12 307 (2005).
[36] G. K. Rozenberg *et al.*, Phys. Rev. B **68**, 064105 (2003).
[37] O. Mathon *et al.*, Phys. Rev. Lett. **93**, 255503 (2004).